Facilitation of Air Traffic Control via OCR-based Aircraft Registration Number Extraction

Dimitrios G. Vidakis[1,2,*], Dimitrios I. Kosmopoulos[3]

[1]Technological Educational Institute Crete, Department of Informatics Engineering, 71004 Heraklion, Greece
[2] Hellenic Air Navigation Services Provider (HANSP) – Hellenic Civil Aviation Authority (HCAA)
[3] University of Patras, Department of Cultural Heritage Management and New Technologies, 30100, Agrinio, Greece

[*] d18c@hcaa.gr

Abstract: To identify any aircraft in the world, it is sufficient to read its registration number. This number is a unique identifier, and offers valuable information, in the same way a car registration number does. In this work we present the results of our feasibility study towards a simple, yet very efficient and effective system to identify aircrafts using video-Optical Character Recognition acquired by off-the-shelf cameras. We used several videos under realistic conditions at the Heraklion airport during high-season and we achieved very promising results. We claim that there is much room for the development of a low-cost airport surface monitoring system based on standard cameras, which can complement high-cost radars.

1. Introduction

In accordance with the International Civil Aviation Organization (ICAO), all aircrafts must be recorded in a national aeronautical authority and must carry proof of such registration (ICAO Annex 7) [1]. Usually an aircraft registration number is printed on a non-flammable plate embedded in the fuselage of the aircraft to specify the identity of the aircraft. This number consists of a prefix, which represents the registration country, and a suffix; these are typically separated by a hyphen (e.g., SX-ARD). According to international air navigation organizations, such as the Federal Aviation Authority (FAA), the registration number is located between the horizontal stabiliser and the wing (Fig. 1).

***Fig. 1**. Registration number position*

Since the location of the registration number is more or less known in advance, it would be feasible to identify it using a low-cost, computer vision system. Application of vision systems to ATM (Air Traffic Management) for detection and identification of aircraft in the vicinity of an airport has been an area of research for some years, see, e.g., [2] [3] [4] [5] [6] [7] [8].

In some cases, identifying an aircraft on the ground is as important as in the air. It's not unusual that the naked eye just isn't enough as demonstrated in Fig. 1, which represents the air traffic controller's view from the airport control tower in Heraklion "Nikos Kazantzakis" International Airport. (Greece) and it needs assistance from machine vision. In the past, a variety of approaches for aircraft identification have been presented. Some of them are quite effective, but they incur high operation costs e.g., [9]. This makes them less attractive, especially for medium to small airports. Even large airports sometimes have a need for supplementary systems in low-coverage areas.

A computer vision system able to identify aircrafts by using their registration number offers a very simple and cost-effective solution. Such a system could serve the control tower and the airport in general, in the following ways:

- monitoring of aircraft movements in the airport;
- fast information delivery to everyone involved;
- monitoring of aircrafts enlisted in 'blacklists';
- monitoring of aircrafts landed unauthorised, e.g., when airports are closed;
- detection of aircraft suspected of any irregularities, such as "emitting noise above permissible limits";
- detection of aircrafts involved in runway incursion incidents.

The contribution of this work is two-fold:

- We present a standalone cost-effective system to monitor online and to identify the registration number of an aircraft in the vicinity of an airport, by using standard cameras and Optical Character Recognition (OCR). As far as we know, such a system does not exist and is innovative. To prove the potential of this method, tests were made using real-life aircraft movements in Heraklion Nikos Kazantzakis Airport in Greece.

• We provide a database of aircraft videos for researchers who wish to extend our results. This is the only such public database that we are aware of.

The following section presents the state of the art on aircraft identification and related applications in airports. Section 3 describes the OCR library and section 4 presents the proposed method. Section 5 presents the experimental results from real life airport traffic. In section 6 there is a discussion about the difficulties of the project. The paper concludes with section 7 stating the possible future developments.

2. Related work

Aircraft identification plays a crucial role in the air and ground traffic control. Several aircraft identification systems have been proposed to address this need. However, most of these systems suffer from high acquisition and maintenance costs. That makes them unaffordable for many medium-to-small airports. Furthermore, even in large airports, which can afford high-tech equipment, there are blind spots created by buildings and other facilities that create gaps in the surface radar image. To fix them by extra radars is rather inefficient. Finally, all of the state-of-the-art systems require the installation of onboard equipment. The most popular such systems are described in the following.

The Surface Movement Radar (SMR) [10] is a system used by air traffic controllers to detect and guide aircrafts and other vehicles on the airport surface. It is the most popular airport surveillance system at the moment. It has high accuracy (7.5m), high scanning frequency (1Hz) and large target detection analysis (below 20 meters). It transmits wavelength pulses with period of 40 nsec, in the band of x-rays or microwaves with very narrow beam (about 0.25o).

The Automatic Dependent Surveillance Broadcast (ADS-B) [11] combines location through Global Navigation Satellite Systems (GNSS) and conventional telecommunication routes between stations. The aircrafts carry special equipment and send their GNSS position combined with flight details to other aircrafts in their area, to the ADS-B ground station and to the corresponding satellite. The combined position data and flight characteristics are transferred to the controller display. This system is considered the most promising system to replace surface radar (SMR).

Due to cost considerations, computer vision systems have been researched, but still their use as aircraft detection/identification or tracking systems is very limited. In the following we present some of the most relevant works.

The INTERVUSE project [12] used video cameras to detect the presence of an aircraft or other vehicles. It used Integrated Radar, Flight plan and digital video data fusion for Advanced – Surface Movement Guidance and Control Systems (A-SMGCS). It could not actually identify aircrafts or their registration number, but it could be potentially helpful as gap filler for a surface radar system. The system was tested in two airports, Manheim Airport and Thessaloniki International Airport. Its main advantages were: (a) The system did not need high data rate between the camera and machine vision processor (MVP), so there was no need for high definition data link. (b) The MVP could control closed loop optical camera such as brightness, gain and electronic zoom. (c) The system was easily portable. Its main drawback was that it needed supplement from surface radar, as well as data from the aircraft's flight plan. Problems were observed when the aircraft remained stationary for a long time, because it incorporated the background and when there were sudden changes in lighting and reduced visibility.

Thirde et al [13] presented a camera network for visual surveillance of the aircraft parking. That system used eight cameras with overlapping recording scenes. The cameras covered mostly the right part of the aircraft, where all processes take place (loading, unloading luggage). The system architecture comprised a scene-tracking section and a scene-understanding section. The scene- tracking section was responsible for detecting, recording and classification of objects of aircraft parking space. The scene-understanding section was responsible for identifying the activities on the ground. This system was presented under AVITRACK (automated surveillance of airport aprons) project. The system was able to recognise the processes and movements of vehicles and people around an aircraft over long periods of time in real time. The results were encouraging, but there were several limitations concerning mainly the detection and identification of moving targets.

Another line of research deals with the aircraft classification using image or radar data, which is different from aircraft identification that we do. Six aircraft types were identified in Dudani [6] using binary images and later Hudson and Psaltis [14] identified 24 aircraft types by using simple correlation measures of radar data. Mitchell and Westerkamp used a statistical approach to extract features from radar data. Straub [8] proposed a scheme for detecting and classifying aircrafts using image features like SIFT/SURF. However it can only be used for aircraft type classification and not and it is only qualitatively evaluated. Saghafi, et al [15] introduced a method of classifying an aircraft by its silhouette using a neural network. They used optical and infrared cameras which recorded images from different distances and view angles. Using a multi-layer neural network and photos from a 3D aircraft model database, over 90% recognition rate in real conditions was achieved.. Similarly, Ali and Choudhry [3] evaluated neural network architectures for detecting and classifying different aircrafts using a video docking system.

Besada, et al [2] is probably the most similar work to ours and its results are also presented in Besada et al [5] and Berlanga et al [4]. It presented a method to identify the aircraft by reading its registration number in high contrast areas using OCR. A database including all identification numbers was additionally used to find the closest match. There are significant differences to our approach. Firstly, [2] assumes that there is a detection system that provides the most relevant image; in their experiments this task was done manually In contrast we relax this requirement, by utilizing the video from the camera, i.e., we are able to locate the spatiotemporal location of the registration number in the video. Secondly, to enhance its performance [2] actually solves a classification problem using a closed set of registration numbers to find the one with the maximum likelihood. This can be very restrictive, because it constantly requires an updated database of valid registration numbers; therefore it requires interconnection with other systems, which in turn increases the installation and maintenance costs. Furthermore [2] is unable to handle aircrafts that seek to avoid identification. Our method does not pose such restrictions, since it does not require any a-priori knowledge about the

available registration numbers. Finally [2] focuses on proposing a custom OCR method, without however providing evidence of any actual benefit compared to other OCR methods. In contrast, we use OCR as a service, thus benefitting from the constantly evolving open source and commercial OCR libraries. Here we describe how to do all the input preprocessing so that such libraries can provide a result close to optimal.

3. The OCR library

To extract the registration number, we use an OCR software library. Here we employ the algorithm of Tesseract open source engine, which is among the most popular open source libraries for OCR [16]. It is based on connected components and blob analysis. Blobs are organised in text lines which are broken into characters depending on their spacing. A final adaptive character classifier is used for providing classification results on both passes.

The OCR function can recognise text within image with a confidence rating, recognise text in regions of interest (ROI / Regions of interest), present words in bounding boxes and confidence rates, find and note text to an image. The input image may grayscale, colour or of binary type. Before starting the recognition process it uses the Otsu thresholding technique for converting the images to binary. For best results the letters have to be higher than 20 pixels and their maximum slope has to be ±10%. The performance of this function is maximised when the text is placed in a uniform background. When the text is in a non-uniform background pre-processing of the image is needed. In the following we analyse how we extract the input to this module, so that it can provide useful results.

At this point we should clarify that the selection of the aforementioned OCR library is by no means restrictive. Any other such library providing similar functionality can be employed as well.

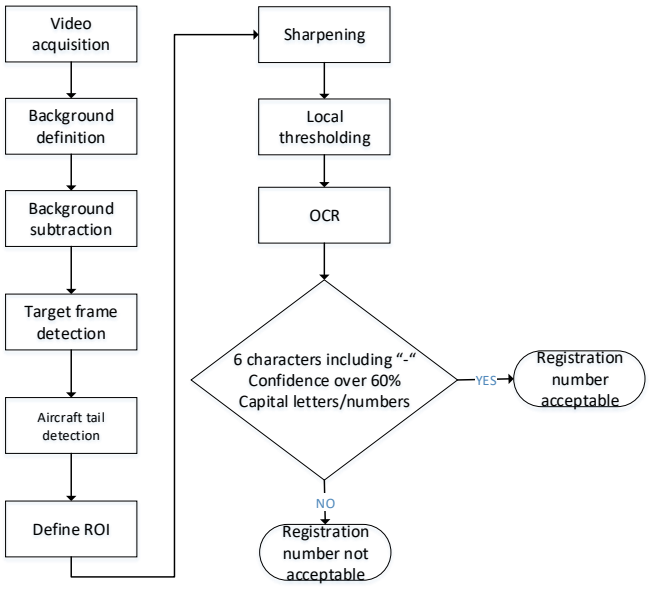

***Fig. 2**. Flow diagram of the proposed method*

4. Proposed methodology

In this section we present the proposed methodology, which is summarized in the flow diagram in Fig. 2. The steps are analysed in the following:

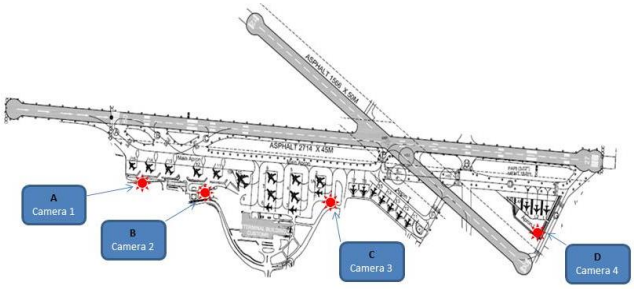

***Fig. 3**. Suggested points of cameras for the Heraklion airport*

Video acquisition. Standard high-definition cameras are used for video acquisition. For a complete coverage several cameras must be deployed in the apron (see Fig. 3). This way there are no blind spots in the area of interest. In our feasibility study we used videos from a single viewpoint, since the results can be easily extended to simultaneous acquisition from multiple viewpoints.

Background definition. The background . (Fig. 4c) is represented by a single frame, which is acquired a few moments before the aircraft shows up in the camera. The background frame is extracted by measuring the amount of motion between consecutive frames, e.g., by simply using the sum of the absolute pixel differences. High motion leads to airplane detection, so we select one of the most recent frames, in which the motion is still close to minimum.

Background Subtraction. The background frame is simply subtracted from every following frame of the video (Fig. 5b), until the sum of the absolute pixel differences drops below a threshold, which signifies the disappearance of the plane. For each of those frames we simply calculate the number of pixels that do not belong to the background (foreground pixels). At this point we should mention that we don't need perfect foreground-background segmentation. We only need to detect the frame giving the maximum amount of foreground pixels, which can be simply extracted by that simple frame subtraction.

Target frame identification. The target frame is the frame with the largest part of the aircraft included. Since the registration number is always close to the vertical tail of the aircraft (fin) we need to focus on this area. The target frame is the one which includes the fin and the largest part of the aircraft. This typically happens when the amount of foreground pixels is maximised. Consequently, the best frame is the one which gives the highest number of foreground pixels when subtracted from the background frame (Fig. 4b, Fig. 5a-b).

Sharpening. A pre-processing is carried out to improve the sharpness of the image, which is crucial for the identification of the registration number characters (Fig. 5c). Here we use the contrast limited adaptive histogram equalization (CLAHE) [15] due to its efficiency and effectiveness. CLAHE operates on small regions in the image, called tiles, rather than the entire image. Each tile's contrast is enhanced, so that the histogram of the output region approximately matches the histogram specified by the cumulative distribution factor (CDF). The neighbouring tiles are then combined using bilinear interpolation to eliminate

artificially induced boundaries. The contrast, especially in homogeneous areas, can be limited to avoid amplifying any noise that might be present in the image.

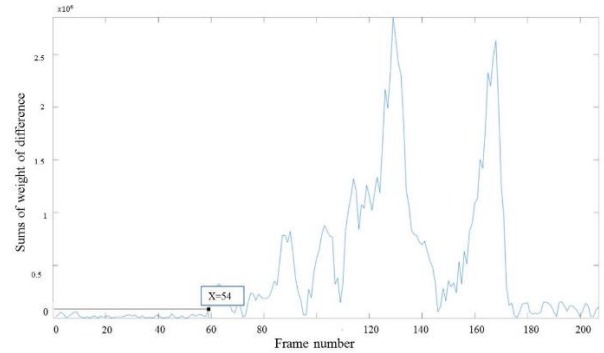

a

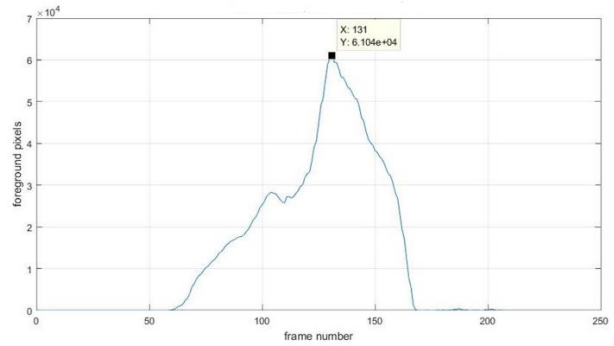

b

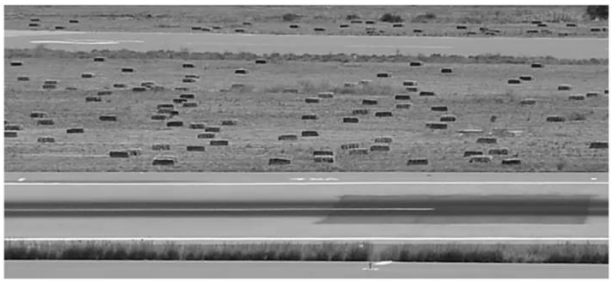

c

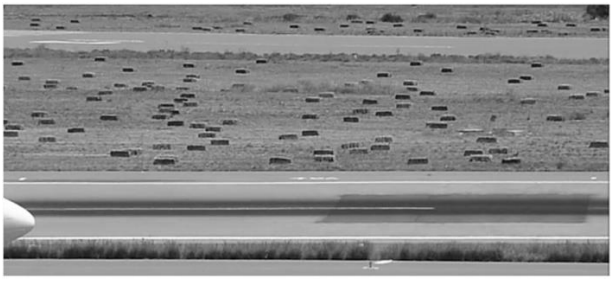

d

Fig. 4*. a. Aircraft detection by consecutive frame difference. The activity is below threshold until frame 54 and increases after that frame. Frame 54 is thus selected as the background frame. The oscillations after frame 175, when the plane is gone, is due to the plane exhaust gas. b. Differences of the current from the background frame (frame 54); the maximum is detected in frame 131 c. the background frame 54 d. The frame 59 in which the plane enters the scene.*

a

b

c

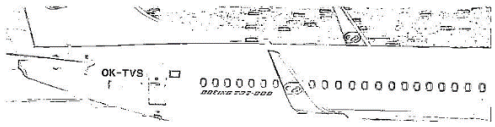

d

Fig. 5 *Detection and processing of the target frame a. The optimal frame b. segmentation from the background c. ROI sharpening d. ROI local thresholding*

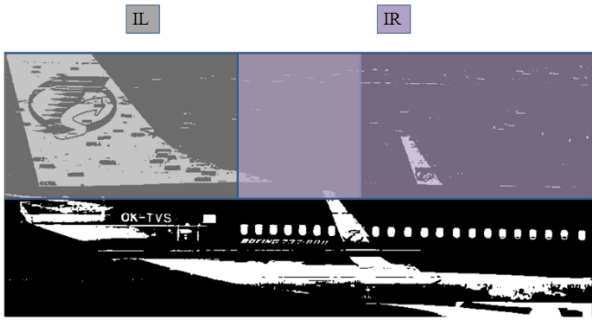

a.

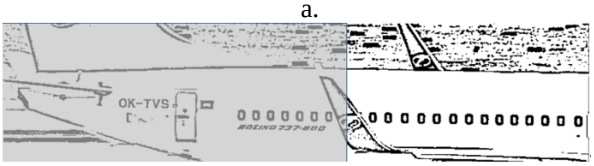

b.

Fig. 6 *a. Upper left (IL) and Upper right (IR) parts of image to be searched for the tail b. Tail image for further processing (shaded)*

Local thresholding with integral images. To segment the registration number, we use an adaptive binarization algorithm which is based on Sauvola local thresholding method [17]. It is used to segment the local structures, such as letters and digits, from the background. It

uses integral images[1] to compute the mean and the variance in local windows. An example is presented in Fig. 5d. We also experimented with Otsu thresholding but the results were disappointing,, because we are not looking for two well separated brightness clusters – as the Otsu method assumes - but for local brightness differences (letters and digits); therefore a local thresholding method is more applicable.

Aircraft tail detection. To limit the region of interest (ROI) and thus the scanning time we need to detect where the tail is. We compare the two upper parts in the image IL and IR (Fig. 6a). The one with the highest amount of foreground pixels contains the vertical tail of the aircraft depending on whether the aircraft goes from left to right or vice versa. This in turn decides which of the two parts (left or right) of the cropped image we will process further (Fig. 6b).

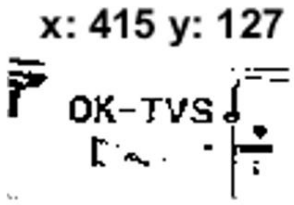

a

```
Possible Registrations and Confidence Percentages
index: 20, conf: 0.82287, words: F-GZTD
index: 21, conf: 0.82287, words: F-GZTD
index: 25, conf: 0.82287, words: F-GZTD
index: 26, conf: 0.82287, words: F-GZTD
index: 27, conf: 0.82287, words: F-GZTD
Aircraft Registration and Origin: F-GZTD
    'France'
```

b

```
Possible Registrations and Confidence Percentages
WARNING: Not able to identify Aircraft Registration
```

c

Fig. 7*. a. Sliding window over registration number b. Successful identification c. unsuccessful identification*

Sliding window size definition. A scanning window is sliding over the selected part in the image reading possible numbers and letters (Fig. 7a)

The size of this scanning window depends on the camera zoom and the distance from the aircraft and can vary (e.g., in our experiment it was from 80x40pixels up to 300x150 pixels (see Table 1, Table 2) depending on the camera and lens type). It is set empirically during the system setup, so that it can include the registration numbers in all cases.

OCR. This function receives as input all sliding windows sequentially. The registration numbers are considered valid when specific rules are satisfied (Fig. 7b-c). These rules are:

a) 6 characters including "-"

b) Confidence over a certain threshold

c) Only capital letters

From these registrations only the most frequently recognised one is accepted as the aircraft's registration number.

Additional services. When we have the aircraft's registration number there are several additional services that can be provided. One of them is to provide the country of the aircraft by associating the identified prefix with a database of country-specific prefixes. For example "SX" refers to Greece, "OO" to Belgium, "G" to Germany and so on.

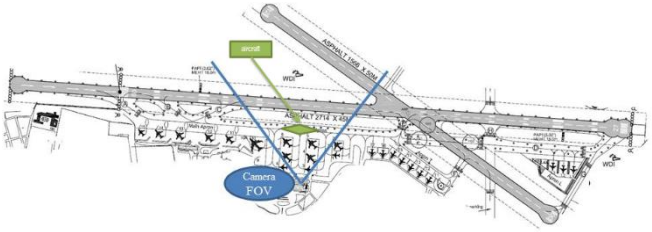

Fig. 8. *Camera Field of view during our experiments in Nikos Kazantzakis Airport of Heraklion*

5. Experimental results

To examine the effectiveness of the algorithm, high definition video of the actual movements of Nikos Kazantzakis airport of Heraklion was recorded. The time period was from May 2015 to August 2017. For each setting a single camera was used, which was installed on the airport control tower (Fig. 8). We used a standard PC (with AMD Phenom II X4 955, operating at 3,2 GHz with 4GB RAM) with the Matlab OCR, which employs the Tesseract library. The cameras used were: Canon EOS 500d, Sony DCR-SR35, Panasonic Lumix DMC-TZ20.

The videos were recorded in daytime and mostly in sunshine. The method is expected to work at night as long as there is appropriate illumination. Clearly, under this setting we expect deterioration of the results under adverse weather conditions such as heavy rain or fog. The target frame is expected to be detected in most cases, however the visibility of the registration number can be seriously affected, and the OCR task can become difficult.

Table 1 presents a sample of successful results of the algorithm. The tail numbers were 100% correctly located after successful detection of the tail, which is the core of the proposed method. The OCR library that we used had a 94.69 % success in identifying the individual characters. 72.5% of the full aircraft registration numbers were perfectly identified. The errors are not due to our method per se, but due to the image quality (affected by installation restrictions of our experimental system) and the employed OCR library. Tesseract was free and easy to integrate, but is known to have problems with noisy images [18]. Other libraries can be used instead (see, e.g., [19] for a list of state-of-the-art OCR software products and their performance evaluation).

The total results are presented in Appendix I. In Table 2 a sample of partially successful results are shown. In this table there some cases of not fully successful registration match. Most common mistakes are shown in Table 3.

[1] An integral image is described as an image in which the intensity at a pixel position is equal to the sum of the intensities of all the pixels above and to the left of that position in the original image

The time spent for video processing during the plane pass varied from 20 to 55 seconds on a standard laptop PC (Intel i5 CPU and 4 GB RAM) using MATLAB. That depended on the identified ROI, which in turn depended on the size of the plane. It also depended on the sliding window size, which in turn depended on the zoom of the camera used in the specific configuration. Sizes between 50x100 and 100x200 pixels were used. We tried to avoid using very big ROIs not only because of performance issues, but also because the flag sign next to the registration number could occasionally confuse the OCR and thus should be better excluded from the ROI.

Our main difference with [2] is that we process the whole video to detect the target frame, which is the one depicting the full tail of the aircraft and we are 100% successful in that. Table 4 shows a detailed comparison of our approach with the one described in [2]. We should note here that the accuracy results are not directly comparable due to the different databases used and due to the fact, that [2] uses prior information about the full set of possible registration numbers, which we don't do.

The videos captured and images from the results can be freely downloaded[2].

***Table 1**: Examples of Successful results. **video (mp4):** The name of the file and also the name of the folder with video and photos from the results found **conf**: the confidence percentage (%) of the result according to ocr command of Matlab. **reg result**: the resulted registration. **correct reg**: the correct registration. **suc**: Success rate (%) reading of the registration. Calculated as a fraction of correct letters out of 6. **country result**: resulted registration*

Video	Conf (%)	Registr. result	Correct Registr.	Country result
AEE_18	79	SX-DVG	SX-DVG	Greece
BER_22	82	D-ABFZ	D-ABFZ	Germany
BER_5	84	HB-IOS	HB-IOS	Switzerland
LLC_9	71	SP-HAF	SP-HAF	Poland
MAV_3	83	SX-MAR	SX-MAR	Greece
TVS_308	78	YL-LCM	YL-LCM	Latvia
CND_301	81	CS-TQU	CS-TQU	Portugal
SWG_2	88	OK-TVV	OK-TVV	Czech Rep.
TRA_5	78	PH-HZJ	PH-HZJ	Netherlands
ELY_401	83	4X-EAK	4X-EAK	Israel
ENT_401	77	SP-ENV	SP-ENV	Poland
FPO_401	83	F-GZTD	F-GZTD	France

6. Discussion

In our experiments, most videos were acquired during daytime with good weather conditions. However, there were several factors that affected adversely the recognition process (see problems in Table 2).

We used off-the-self consumer cameras, with rather cheap lenses, which did not facilitate optimal video capture. The camera was placed inside the air traffic control tower due to available space for testing and calibrating. The optimum and also suggested spot is on board the light poles in the airport apron. Thus, there always be enough light to capture the requested video. This wasn't possible to put to test for the time being since due to restrictions by the Civil Aviation Authorities. By installing the cameras on the light poles we can achieve weather immunity, since even fog or heavy rain or even night time could do little to lower the recognition results. This is due to the proximity of the camera and taxing aircraft (about 80 to 100m). Given the fact that few airports in the world have the facilities to allow an aircraft landing with visibility with less than 200 meters (Runway Visibility Range <200m), this prospect covers many airports worldwide.

***Table 2**: Partially successful results. **video (mp4):** The name of the file and also the name of the folder with video and photos from the results found **conf**: the confidence percentage (%) of the result according to ocr command of Matlab. **reg result**: the resulted registration. **correct reg**: the correct registration. **suc**: Success rate (%) reading of the registration. Calculated as a fraction of correct letters out of 6. **country result**: resulted registration country. **correct country**: correct registration country.*

Video	Conf (%)	Reg result	Correct Reg	Country result	Correct Country
AEE_12	71	SX-DEF	SX-DGF	Greece	Greece
AEE_6	66	SK-DVD	SX-DVQ	-	Greece
BAL_2	75	VL-BBS	YL-BBS	-	Latvia
BIE_2	81	F-GVAD	F-GVAO	France	France
EXS_4	65	E-ASXE	D-ASXB	-	Germa-ny
EZY_5	83	G-EZDL	G-EZOL	UK	UK
ORE_101	73	VD-IWJ	VQ-BWJ	-	Turcs & Caicos
LLC_201	77	LY-SFG	LY-SPG	Lithua-nia	Lithua-nia
AFL_201	76	VD-BWE	VQ-BWE	-	Turcs & Caicos
TVS_307	760	UK-TVF	OK-TVP	Uzbeki-stan	Austria

Moreover, the tower glass anti-sun membranes reduced the sharpness of the video. This could be avoided by mounting the camera on the exterior of the control tower. However, that could cause vibrations in many cases due to wind, therefore a good fixation would be required.

The angle of reception was many times to blame for some poor results. The optimum angle would be within the

[2] The following link is provided for review purposes, (a more official link will be given upon acceptance). https://drive.google.com/open?id=0B7ovGz8kDXBibnFnX1ppTkVfSlE

$90\pm10^{\circ}$ angle field of view relative to the aircraft movement but many times this wasn't feasible due to obstacles (parked aircraft and other vehicles in the apron).

To achieve optimum results some additional points have to be noticed. The taxiing aircraft's view should at no time be affected by parked aircrafts, while other aircraft lights should not occlude the camera, e.g., when they exit from the runway. Another factor is the speed of the aircraft, that must be relevant to the sampling of the camera so that satisfactory images are produced. (About 25fps - 40knots). The speed limit in the apron for the aircrafts is 20 knots.

In practice, considering the above restrictions, the results were quite satisfactory. Under most circumstances, during the day, with both high definition cameras (HD) an average 78.43% confidence that the registration number was found, was achieved and managed to read the digits in the right order in 94.69% of cases.

Table 3: *Most common mistakes*

Correct digit	Mistaken for
O	U, D
Q	D
X	A, K, E
B	E
V	Y
P	F
S	E
5	S

7. Conclusion and future work

We proposed a computer vision-based system for the identification of aircraft registration numbers in the airport environment. Taking into account the minimum system requirements (off-the-shelf cameras with a standard PC running rather simple code), the system may provide a very cheap alternative to expensive aircraft identification systems. This feasibility study may motivate the development of more elaborate systems towards this direction.

Some of the possible future developments may be:

- Use of a fixed position video recording system specialised for monitoring moving objects.
- Development and testing for operation under adverse weather conditions.
- Development of user-friendly interface.
- Integration with airport collaborative decision-making systems to confirm registration numbers and optimise results, eventually using voice data from the control tower, to produce a complete picture of traffic at an airport.
- Implementation of camera network in an airport to achieve full area, real time registration scanning and consequently produce a low-cost airport surface movement ground control system.

REFERENCES

[1] "ICAO," INTERNATIONAL CIVIL AVIATION ORGANIZATION, 2015. [Online]. Available: http://www.icao.int.

[2] A. Berlanga, J. A. Besada, J. G. Herrero, J. M. Molina, J. I. Portillo and J. R. Casar, "Aircraft identification integrated into an airport surface surveillance video system," Machine Vision and Applocations, vol. 15, no. No. 3, pp. 164-171, July 2004.

[3] S. Ali and M. Choudhry, "A generalized higher order neural network for aircraft recognition in a video docking system," Neural Comput & Applic, pp. 19-21, 2010.

[4] A. Berlanga, J. Garcia-Herrero, J. Molina, J. Besada and J. Portillo, "OCR parameters tuning by means of evolution strategies for aircraft's tail number recognition," in Evolutionary Computation, Honolulu, 2002.

[5] J. Besada, J. Garcia, M. Portillo, M. J., A. Varona and G. Gonzalez, "Airport surface surveillance based on video images," IEEE Transactions on Aerospace and Electronic systems, vol. 41, no. 3, pp. 1075-1082, July 2005.

[6] S. Dudani, K. Breeding and R. McGhee, "Aircraft Identification by Moment Invariants," IEEE Transactions on Computers, Vols. C-26, no. 1, pp. 39-46, Jan. 1977.

[7] N. Pavlidou, N. Grammalidis, K. Dimitropoulos, D. Simitopoulos, A. Gilbert, E. Piazza, C. Herrlich, R. Heidger and M. Strintzis, "IST INTERVUSE project: Intergrated radar, flight plan and digital video data fusion for A-SMGCS," in ITS in Europe Congress, Budapest, 2004.

[8] S. Jeremy, "Application of an image feature network-based object recognition algorithm to aircraft detection and classification," in Automatic Target Recognition XXIV, Baltimore, Maryland, US, 2014.

[9] Eurocontrol, "Advanced Surface Movement Guidance and Control System (A-SMGCS)," 2013. [Online]. Available: http://www.skybrary.aero.

[10] Eurocontrol, "Surface Movement Radar," ACDM. [Online].

[11] Eurocontrol, "Automatic Dependent Surveillance Broadcast (ADS-B)," [Online].

[12] "INTERVUSE," Intergrated Radar, Flight Plan and Digital Video Data Fusion for SMGCS, 2012. [Online]. Available: http://www.iti.gr/intervuse.

[13] D. Thirde, M. Borg and J. Ferryman, "A Real-Time Scene Understanding System for Airport Apron Monitoring," ORION Group, INRIA Sophia-Antipolis, France, 2004.

[14] S. Hudson and D. Psaltis, "Correlation filters for aircraft identification from radar range profiles," IEEE Trans. on Aerospace and Electronic Systems, 29(3), 741-748, 1993.

[15] F. Saghafi, S. M. Khansari Zadeh and V. Etminan Bakhsh, "Aircraft Visual identification by neural networks," J. of Aerospace Science and Technology, 5(3), 123-128, 2008.

[16] Ray Smith, "An Overview of the Tesseract OCR Engine," in Int. Conference on Document Analysis and Recognition, 2007.

[17] F. Shafait, D. Keysers and B. B. Thomas, "Efficient Implementation of Local Adaptive Thresholding Techniques Using Integral Images," 2008.

[18] Helinski, M., Kmieciak, M., Parkola, T., 2012. Report on the comparison of Tesseract and ABBYY FineReader OCR engines, IMPACT technical report, 2012

[19] A. Rivera, Best document scanning services, [Online]. Available: https://www.business.com/categories/document-scanning-services/

8. Appendix I

Table 4a *The full results for the whole database*

	video (mp4)	Reg Result		correct registration	success (:/6 digits) %	country result	correct country
1	**AEE_12**	SX-DEF	71,00%	SX-DGF	**83,33%**	Greece	Greece
2	**AEE_18**	SX-DVG	79,00%	SX-DVG	**100,00%**	Greece	Greece
3	**AEE_19**	SX-DGI	81,00%	SX-DGI	**100,00%**	Greece	Greece
4	**AEE_2**	SX-DST	73.56%	SX-DGT	**83,33%**	Greece	Greece
5	**AEE_20**	SX-DVX	76,00%	SX-DVX	**100,00%**	Greece	Greece
6	**AEE_29**	SX-DES	72,00%	SX-DGS	**83,33%**	Greece	Greece
7	**AEE_6**	SK-DVD	66,36%	SX-DVQ	**66,67%**	-	Greece
8	**AEE_9**	SX-DVV	75,00%	SX-DVV	**100,00%**	Greece	Greece
9	**AFL_2**	VP-BUS	73,00%	VP-BOS	**83,33%**	Bermuda	Bermuda
10	**ALS_1**	EC-LNC	87,00%	EC-LNC	**100,00%**	Spain	Spain
11	**BAL_2**	VL-BBS	75,00%	YL-BBS	**83,33%**	-	Latvia
12	**BBG_1**	EX-TLE	70,00%	SX-TZE	**66,67%**	Kyrgyzstan	Greece
13	**BER_22**	D-ABFZ	82,50%	D-ABFZ	**100,00%**	Germany	Germany
14	**BER_5**	HB-IOS	84,00%	HB-IOS	**100,00%**	Switzerland	Switzerland
15	**BER_6**	HB-XOF	60,00%	HB-IOP	**66,67%**	Switzerland	Switzerland
16	**BIE_1**	F-GVAP	75,00%	F-GVAP	**100,00%**	France	France
17	**BIE_2**	F-GVAD	81,00%	F-GVAO	**83,33%**	France	France
18	**BIE_8**	F-HCOA	76,00%	F-HCOA	**100,00%**	France	France
19	**CFG_6**	D-AJCF	66,50%	D-AICF	**83,33%**	Germany	Germany
20	**CFG_8**	D-AICL	75,00%	D-AICL	**100,00%**	Germany	Germany
21	**EDW_6**	HB-IHZ	83,00%	HB-IHZ	**100,00%**	Switzerland	Switzerland
22	**EXS_4**	E-ASXE	65,00%	D-ASXB	**66,67%**	-	Germany
23	**EZY_5**	G-EZDL	83,00%	G-EZOL	**83,33%**	UK	UK
24	**FPO_6**	F-GZTC	80,00%	F-GZTC	**100,00%**	France	France
25	**LLC_5**	SP-HAF	75,00%	SP-HAF	**100,00%**	Poland	Poland
26	**LLC_7**	SP-HAG	72,00%	SP-HAG	**100,00%**	Poland	Poland
27	**LLC_8**	SP-HAD	74,00%	SP-HAD	**100,00%**	Poland	Poland
28	**LLC_9**	SP-HAF	71,00%	SP-HAF	**100,00%**	Poland	Poland
29	**MAV_3**	SX-MAR	83,00%	SX-MAR	**100,00%**	Greece	Greece
30	**SEH_1**	SX-LDS	83,00%	SX-LOS	**83,33%**	Greece	Greece
31	**SWG_2**	OK-TVV	88,00%	OK-TVV	**100,00%**	Czech Republic	Czech Republic
32	**TCW_1**	OD-TCV	81,00%	OO-TCV	**83,33%**	Lebanon	Austria
33	**TFL_1**	PH-HZG	84,00%	PH-HZG	**100,00%**	Nederlands	Nederlands
34	**TOM_2**	G-DBVF	77,00%	G-OBYF	**66,67%**	UK	UK
35	**TOM_3**	G-TAID	68,00%	G-TAWD	**83,33%**	UK	UK
36	**TRA_5**	PH-HZJ	78,00%	PH-HZJ	**100,00%**	Nederlands	Nederlands

Table 4b *The full results for the whole database*

37	**TRA_6**	F-GZHB	85,00%	F-GZHB	**100,00%**	France	France
38	**TRA_7**	PH-HZJ	86,00%	PH-HZJ	**100,00%**	Nederlands	Nederlands
39	**TRA_8**	PH-HZJ	82,00%	PH-HZJ	**100,00%**	Nederlands	Nederlands
40	**TUI_10**	D-ATUQ	63,00%	D-ATUQ	**100,00%**	Germany	Germany
41	**TUI_13**	D-ATUI	80,00%	D-ATUI	**100,00%**	Germany	Germany
42	**TUI_32**	D-ANLK	78,00%	D-AHLK	**83,33%**	Germany	Germany
43	**TUI_34**	D-ABKI	69,00%	D-ABKI	**100,00%**	Germany	Germany
44	**TUI_35**	D-AMFV	77,00%	D-AHFV	**83,33%**	Germany	Germany
45	**TUI_6**	G-TAII	75,00%	G-TAWI	**83,33%**	Germany	Germany
46	**TUI_7**	D-AEKI	69,00%	D-ABKI	**83,33%**	Germany	Germany
47	**TVS_1**	OK-TVS	83,00%	OK-TVS	**100,00%**	Czech Republic	Czech Republic
48	**TVS_31**	OK-YVS	73,00%	OK-TVS	**83,33%**	Czech Republic	Czech Republic
49	**TVS_4**	OK-TSJ	79,00%	OK-TSJ	**100,00%**	Czech Republic	Czech Republic
50	**TVS_4**	OK-TSJ	84,00%	OK-TSJ	**100,00%**	Czech Republic	Czech Republic
51	**XLF_11**	F-HAXL	79,00%	F-HAXL	**100,00%**	France	France
52	**XLF_4**	F-HAXL	78,00%	F-HAXL	**100,00%**	France	France
53	**TVS_102**	OK-TVM	70,00%	OK-TVM	**100,00%**	Czech Republic	Czech Republic
54	**ORE_101**	VD-IWJ	73,00%	VQ-BWJ	**66,67%**	-	Turcs & Caicos
55	**LLC_201**	LY-SFG	77,00%	LY-SPG	**83,33%**	Lithuania	Lithuania
56	**AFL_201**	VD-BWE	76,00%	VQ-BWE	**83,33%**	-	Turcs & Caicos
57	**AEE_301**	SX-DVU	78,00%	SX-DVU	**100,00%**	Greece	Greece
58	**AEE_302**	SX-DVG	82,00%	SX-DVG	**100,00%**	Greece	Greece
59	**AEE_303**	SX-DGE	77,00%	SX-DGE	**100,00%**	Greece	Greece
60	**AEE_306**	SX-DVH	84,00%	SX-DVH	**100,00%**	Greece	Greece
61	**AEE_307**	SX-DVI	79,00%	SX-DVW	**83,33%**	Greece	Greece
62	**AEE_310**	SX-DVT	74,00%	SX-DVY	**83,33%**	Greece	Greece
63	**AEE_311**	SX-DVM	70,00%	SX-DVM	**100,00%**	Greece	Greece
64	**AEE_203**	SX-DVY	79,00%	SX-DVY	**100,00%**	Greece	Greece
65	**AEE_205**	SX-DEV	73,00%	SX-DGV	**83,33%**	Greece	Greece
66	**AUA_302**	OE-LDE	86,00%	OE-LDE	**100,00%**	Austria	Austria
67	**BEL_301**	OO-SNG	76,00%	OO-SNG	**100,00%**	Belgium	Belgium
68	**BER_302**	D-AECK	71,00%	D-ABCK	**83,33%**	Germany	Germany
69	**BMS_201**	YR-AMB	79,00%	YR-AMB	**100,00%**	Romania	Romania
70	**BMS_302**	VR-AMB	80,00%	YR-AMB	**83,33%**	-	Romania
71	**BPA_301**	I-EPAG	79,00%	I-BPAG	**83,33%**	Italy	Italy
72	**CND_301**	CS-TQU	81,00%	CS-TQU	**100,00%**	Portugal	Portugal
73	**DLH_301**	D-AIPC	80,00%	D-AIPC	**100,00%**	Germany	Germany
74	**ELB_301**	LY-GGC	67,00%	LY-GGC	**100,00%**	Lithuania	Lithuania
75	**ELB_302**	LY-GGC	73,00%	LY-GGC	**100,00%**	Lithuania	Lithuania
76	**EXS_201**	D-ASXK	76,00%	D-ASXK	**100,00%**	Germany	Germany

Table 4c *The full results for the whole database*

77	**EZY_301**	G-EZBM	73,00%	G-EZBM	**100,00%**	UK	UK
78	**FPO_302**	F-GZTA	85,00%	F-GZTA	**100,00%**	France	France
79	**GWI_301**	D-AIPY	70,00%	D-AIPY	**100,00%**	Germany	Germany
80	**ISS_301**	EI-FFK	75,00%	EI-FFK	**100,00%**	Eire	Eire
81	**LLC_301**	D-ASPG	70,00%	D-ASPG	**100,00%**	Germany	Germany
82	**LLC_303**	LY-ONJ	85,00%	LY-ONJ	**100,00%**	Lithuania	Lithuania
83	**SEH_303**	SX-LUS	82,00%	SX-LOS	**83,33%**	Greece	Greece
84	**SEH_304**	SA-DIQ	58,00%	SX-DIQ	**83,33%**	-	Greece
85	**SEH_305**	SX-DIQ	80,00%	SX-DIQ	**100,00%**	Greece	Greece
86	**SVR_302**	VD-BSR	74,00%	VQ-BSR	**83,33%**	-	Bermuda
87	**TCW_301**	G-TCDN	81,00%	G-TCDN	**100,00%**	UK	UK
88	**TRA_302**	PH-HZJ	85,00%	PH-HZJ	**100,00%**	Nederland	Nederland
89	**TUI_303**	D-ATUE	77,00%	D-ATUC	**83,33%**	Germany	Germany
90	**TUI_304**	D-ATUP	79,00%	D-ATUP	**100,00%**	Germany	Germany
91	**TVS_301**	YL-LCD	79,00%	YL-LCD	**100,00%**	Latvia	Latvia
92	**TVS_305**	G-FJVE	79,00%	G-FJVE	**100,00%**	UK	UK
93	**TVS_307**	UK-TVF	76,00%	OK-TVP	**66,67%**	Uzbekistan	Austria
94	**TVS_308**	YL-LCM	78,00%	YL-LCM	**100,00%**	Latvia	Latvia
95	**AEE_401**	SX-DVM	80,00%	SX-DVM	**100,00%**	Greece	Greece
96	**AEE_402**	SX-DVU	85,00%	SX-DVU	**100,00%**	Greece	Greece
97	**AEE_403**	SX-DGN	79,00%	SX-DGN	**100,00%**	Greece	Greece
98	**AEE_406**	SX-DVS	84,00%	SX-DVS	**100,00%**	Greece	Greece
99	**AEE_407**	EX-DGL	75,00%	SX-DGL	**83,33%**	Kyrgyzstan	Greece
100	**BAL_401**	G-GATL	76,00%	G-GATL	**100,00%**	UK	UK
101	**COB_401**	SB-DCR	80,00%	5B-DCR	**83,33%**	-	Cyprus
102	**ELY_401**	4X-EAK	83,00%	4X-EAK	**100,00%**	Israel	Israel
103	**ENT_401**	SP-ENV	77,00%	SP-ENV	**100,00%**	Poland	Poland
104	**FPO_401**	F-GZTD	83,00%	F-GZTD	**100,00%**	France	France
105	**AEE_801**	SX-DGX	84,00%	SX-DGX	**100,00%**	Greece	Greece
106	**AEE_802**	SX-DVW	78,00%	SX-DVW	**100,00%**	Greece	Greece
107	**AEE_803**	SX-DVM	78,00%	SX-DVM	**100,00%**	Greece	Greece
108	**AEE_807**	SX-DGZ	81,00%	SX-DGZ	**100,00%**	Greece	Greece
109	**AEE_811**	SX-DVJ	89,00%	SX-DVJ	**100,00%**	Greece	Greece
110	**AEE_812**	SX-DGJ	89,00%	SX-DGJ	**100,00%**	Greece	Greece
111	**AVL_001**	YU-ANJ	91,00%	YU-ANJ	**100,00%**	Serbia	Serbia
112	**BBG_901**	9H-TAS	81,00%	9H-TAS	**100,00%**	Malta	Malta
113	**BBG_902**	9H-TAS	82,00%	9H-TAS	**100,00%**	Malta	Malta
114	**BEL_801**	OO-SSI	85,00%	OO-SSI	**100,00%**	Belgium	Belgium
115	**ELB_701**	LY-LGC	81,00%	LY-LGC	**100,00%**	Lithuania	Lithuania
116	**ELB_703**	LY-GGC	90,00%	LY-GGC	**100,00%**	Lithuania	Lithuania
117	**EZY_801**	G-EZTM	81,00%	G-EZTM	**100,00%**	UK	UK

Table 4d *The full results for the whole database*

118	**EZY_802**	G-EZTM	77,00%	G-EZTM	**100,00%**	UK	UK
119	**FPO_501**	F-GZTM	83,00%	F-GZTM	**100,00%**	France	France
120	**FPO_502**	F-GZTS	77,00%	F-GZTS	**100,00%**	France	France
121	**FPO_503**	F-GZTS	82,00%	F-GZTS	**100,00%**	France	France
122	**GMI_801**	D-ASTF	77,00%	D-ASTF	**100,00%**	Germany	Germany
123	**GMI_802**	D-ASTU	86,00%	D-ASTU	**100,00%**	Germany	Germany
124	**TRA_803**	F-HTVB	76,00%	F-HTVB	**100,00%**	France	France
125	**STE_101**	YR-SEA	87,00%	YR-SEA	**100,00%**	Romania	Romania
126	**TRA_805**	PH-HZO	85,00%	PH-HZO	**100,00%**	Nederlands	Nederlands
127	**TRA_806**	PH-GUV	86,00%	PH-GUV	**100,00%**	Nederlands	Nederlands
128	**TRA_807**	F-GZHR	84,00%	F-GZHR	**100,00%**	France	France
129	**TUI_803**	G-OBYE	74,00%	G-OBYE	**100,00%**	UK	UK
130	**TVS_801**	OK-TVO	74,00%	OK-TVO	**100,00%**	Czech Republic	Czech Republic
131	**TVS_808**	OM-GTF	85,00%	OM-GTF	**100,00%**	Slovakia	Slovakia
132	**UTA_001**	VP-BVL	90,00%	VP-BVL	**100,00%**	Bermuda	Bermuda
133	**AUA_901**	OE-LBS	92,00%	OE-LBS	**100,00%**	Austria	Austria
134	**BBG_911**	9H-TAS	72,00%	9H-TAS	**100,00%**	Malta	Malta
135	**ELB_901**	LY-GGC	84,00%	LY-GGC	**100,00%**	Lithuania	Lithuania
136	**AZA_901**	VQ-BJK	78,00%	VG-BJK	**83,33%**	-	Bermuda
137	**AZI_901**	LZ-CGW	70,00%	LZ-CGW	**100,00%**	Bulgaria	Bulgaria
138	**EXS_901**	D-ASXU	80,00%	D-ASXQ	**83,33%**	Germany	Germany
139	**LLC_901**	SP-HAG	81,00%	SP-HAG	**100,00%**	Poland	Poland
140	**LLC_904**	OK-TVL	91,00%	OK-TVL	**100,00%**	Czech Republic	Czech Republic
141	**TVS_807**	OM-GTF	72,00%	OM-GTF	**100,00%**	Slovakia	Slovakia
142	**EXS-903**	VQ-BJK	84,00%	VQ-BJK	**100,00%**	Bermuda	Bermuda
143	**AEE_905**	SX-DVR	78,00%	SX-DVR	**100,00%**	Greece	Greece
144	**AEE_906**	SX-DGS	78,00%	SX-DGS	**100,00%**	Greece	Greece
145	**BBG_903**	9H-TAS	88,00%	9H-TAS	**100,00%**	Malta	Malta
146	**BBG_904**	9H-NOA	85,00%	9H-NOA	**100,00%**	Malta	Malta
147	**BEL_901**	OO-SSM	75,00%	OO-SSM	**100,00%**	Belgium	Belgium
148	**BPA_901**	EI-CSI	88,00%	EI-CSI	**100,00%**	Eire	Eire
149	**CND_902**	PH-HSF	78,00%	PH-HSF	**100,00%**	Nederlands	Nederlands
150	**EWG_902**	D-AEER	50,00%	D-AEWR	**83,33%**	Germany	Germany
151	**EXS_905**	D-ASXA	78,00%	D-ASXA	**100,00%**	Germany	Germany
152	**EZY_901**	3-EZPV	73,00%	G-EZPV	**83,33%**	-	UK
153	**NLY_901**	HB-JOX	87,00%	HB-JOX	**100,00%**	Switzerland	Switzerland
154	**NWS_906**	VG-BDZ	78,00%	VQ-BDZ	**83,33%**	-	Bermuda
155	**TRA_903**	F-GZHY	85,00%	F-GZHY	**100,00%**	France	France
156	**TRA_904**	PH-HZJ	70,00%	PH-HZJ	**100,00%**	Nederlands	Nederlands
157	**TUI_801**	G-TAWS	86,00%	G-TAWS	**100,00%**	UK	UK
158	**WHI_102**	ES-SAO	86,00%	ES-SAQ	**83,33%**	Estonia	Estonia

Table 4e *The full results for the whole database*

159	**WHI_104**	SE-RKA	78,00%	SE-RKA	**100,00%**	Sweden	Sweden
160	**AEE_804**	SX-DVH	74,00%	SX-DVW	**83,33%**	Greece	Greece